

Influence of Urban Rail Transit on Corrosion of Buried Steel Gas Pipeline

Jianguo Feng, Zhiguang Chen, Yitong Xie, Cong Wu, Chaokui Qin*

Department of Mechanical and Energy Engineering, Tongji University, Shanghai 201804, China

*E-mail: chkqin@tongji.edu.cn.

Received: 26 January 2021 / Accepted: 20 March 2021 / Published: 30 April 2021

It has been established that the operation of direct current (D.C.) rail traction systems can cause severe corrosion to neighbouring steel pipelines buried near rail buttresses. In this paper, a novel measurement device was developed to record the pipe-to-soil potential, surface potential gradient, and pipeline current of steel pipelines located in the vicinity of Shanghai rail transit line 1, Fujin Road Station. The results show that the pipe-to-soil potential fluctuated within -2.04 V~1.855 V, the averaged surface potential gradient was 12.18 mV/m, and its direction was 30.2 degrees southeast during rail transit operation. The current within the pipeline turned out to be -40 mA~37 mA and the entering current is 4 times stronger than the leaving current. The comparison of measured data corresponding to periods of rail transit operation and no operation clearly revealed that the interference comes from rail traction. Finally, measures to mitigate this interference were proposed, including insulation joints, drainage devices, smart monitoring systems, etc. The work in this paper can therefore help protect the steel pipeline that was buried near the rail buttress from stray current corrosion during municipal construction processes.

Keywords: rail transit; rail buttress; pipeline corrosion; testing device; stray current

1. INTRODUCTION

Accompanied by accelerating urbanization processes, an increasing number of people are moving to large cities, and as a result, serious traffic-related issues have arisen. To alleviate these issues, various kinds of rail transit have been constructed in mid-sized cities and metropolises. Unfortunately, with increasing operating mileages and limited underground space [1], rail transit inevitably intersects with or runs parallel to underground steel pipelines [2]. Meanwhile, due to the current level of project construction and rail transit technological development, the driving current of direct current (D.C.) rail transit locomotives always contains a portion that cannot be returned to the substation [3], resulting in driving current leakage. The leaked current inevitably flows to the soil through the tracks or rail buttresses [4] and further flows to neighbouring buried steel pipelines with anti-corrosion coating

defects. Depending on the presence of suitability corrosive soil containing oxygen and water, electrochemical reactions between the charged steel pipe-section and soil with oxygen and water may occur and cause corrosion damage to the steel pipe-section in locations with damaged coating [5, 6]. More notably, with the increased operating time of the rail transit system, pipeline corrosion gradually increases, which may eventually cause leakage accidents, such as pipeline perforations or explosions. Small pipeline leakage incidents may prevent the surrounding residents from temporarily using natural gas, which can act as an inconvenience to daily operation, while serious pipeline leakage incidents may cause property losses, casualties, environmental pollution issues, etc. [7].

To minimize pipeline leaking incidents, it is necessary to periodically monitor the operation status of pipelines, so that pipeline corrosion risks can be evaluated. Currently, some researchers, including Allahkaram [8], Chen [3], and Li [9], have evaluated pipeline corrosion by measuring the pipe-to-soil potential of steel rails. However, this method does not directly provide parameters relevant to corrosion, such as the pipe-to-soil potential and the current within the pipeline, leading to an inaccurate evaluation of the degree corrosion suffered by pipelines. Although some researchers have measured the potential to evaluate pipeline corrosion, such as Iranian researcher Allahkaram [8]. The influence of current leakage along-track buttresses has not been studied, in recent years, some researchers, such as Chen [3, 10], have conducted field testing on buried pipelines, but the involved equipment has usually been based on wired data acquisition, and this method can not be used in complex field tests [11, 12].

In this paper, a new device integrated with remote data transmission was developed to measure corrosion-related parameters, including the pipe-to-soil potential, surface potential gradient, and current within the pipeline, of the buried steel pipes located near rail buttresses. The D.C. stray current interference was evaluated by analysing the measured data. Finally, three methods are proposed to mitigate D.C. interference and improve pipeline protection against steel pipelines on the sides of the rail buttresses.

2. EXPERIMENTAL

2.1 Corrosion principle

Currently, the D.C. voltage of driving urban rail transit locomotives is generally 1500/750 V. Such a high operating voltage is certain to have a large current flowing into and out of the substation. However, during locomotive operation, the entire driving current coming from the substation cannot be returned to the substation, thereby inevitably flowing towards the soil with the help of the rail buttress. The process of current leakage is shown in Figure .1. First, the current leaking from the rail (stray current) flows into the soil through the buttress, and the current flowing from the rail to the buttress is carried out by electrons. The electrons migrate to the soil via the steel bars inside the rail buttress. When the current flows to the buttress, under the action of an electrical field force, the electrons near the contact interface between the buttress and the soil move away from the contact interface, causing the potential difference at the buttress-soil contact interface to increase, thereby driving the positive ions in the soil to migrate away from the interface, and the negative ions to migrate close to the interface. Due to the migration of positive and negative ions, a current is generated in the soil. As the migration process proceeds, there

are more positive ions and fewer negative ions near the surface of the buried steel pipelines, which changes the electric field distribution running along the surface. The electrons on the steel pipeline are moved to balance the potential difference of the steel surface caused by the movement of positive and negative ions in the soil. Therefore, the leaked current coming from the rail buttress flows into the pipeline. Whether the anti-corrosion coating of the buried steel pipeline is damaged due to construction issues or long-term disrepair, the current in the pipeline outflows from the damaged position to be returning to the substation. Meanwhile, the current backflow process also needs to move through three processes, including the migration of electrons and ions at the interface between the buried pipeline and the soil due to electrical field forces, the migration of positive and negative ions in the soil, and the movement of electrons and ions between the rail buttress and the soil interface due to electrical field forces. The migration principle of electrons and ions in this process is the same as that of a leaked current flowing into the pipeline, but the direction of the electrical field is opposite to the movement direction of electrons and ions. It is worth noting that at the interface where the current flows out of the surface of the steel pipeline, the existence of water, oxygen, and other components may cause pipeline corrosion. The electrochemical reaction equations of the sensing cathode and anode are shown in equations (1) and (2) as follows.

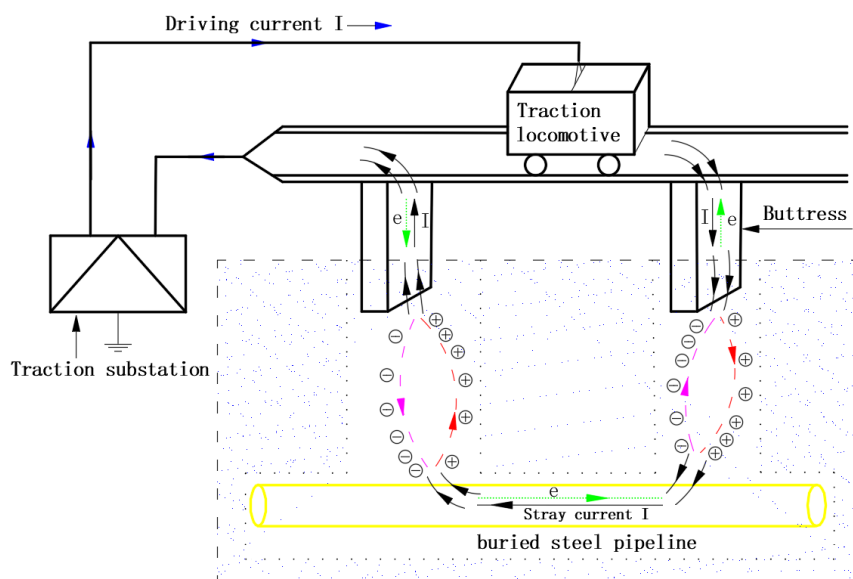
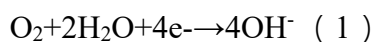


Figure 1. Schematic diagram of the electron-ion migration principle between the rail buttress and a steel pipeline

2.2 Testing device

The test device consisted of a computer, a data acquisition module (AD7606 ADC with 16bit), a data processing module (Raspberry Pi 3 Model B+), a wireless remote module (E840- DTU (GPRS-03)), a set of copper sulfate reference electrodes, and a small portable lithium battery power supply, as

well as other components. The acquisition module has the characteristics of including 16 bits, 8 channels, and a maximum sampling frequency of 200 Ksps. The wireless remote module is supplied with a power supply voltage in the range of 8~28 V and adopted by two power supply modes, including a D.C. power supply and a terminal block, the maximum speed of which is 85.6 kbps for uploading and downloading the data. The operating procedure is implemented in Python, and the device can realize the functions of real-time data upload and automatic storage.

2.3 Field testing

During the time period between 17:00 and 00:10, the novel wireless testing device conducts corrosion analysis of the rail transit interference on a buried steel gas pipeline located near the rail buttress of Fujin Road Station of Shanghai rail transit line 1. The rail transit locomotives are not operated along this line within the time period of 23:50~00:10. Figure.2 shows the arrangement of the field-testing apparatus. The track runs parallel to the unmeasured buried steel gas pipeline, and the vertical distance is 20 metres between the rail buttress and the gas pipeline. The pipeline is located on the east side of the rail transit line 1, and the test station of the gas pipeline to the southeast of the rail buttress. The vertical and parallel distances from the station to line 1 and the buttress are 20 and 10 metres, respectively, as shown in Figure.2. The burial depth of the pipeline is 2 metres, the pipeline diameter is 500 mm, and the internal pressure of the pipeline is 0.65 MP. The aforementioned device measures the pipe-to-soil potential, surface potential gradient, and current within the pipeline during the transit period of the locomotives. According to the Chinese standard GB/T19285-2014 [13], cathodic protection equipment should be cut off 24 hours before field testing to ensure that it does not interfere with the test results.

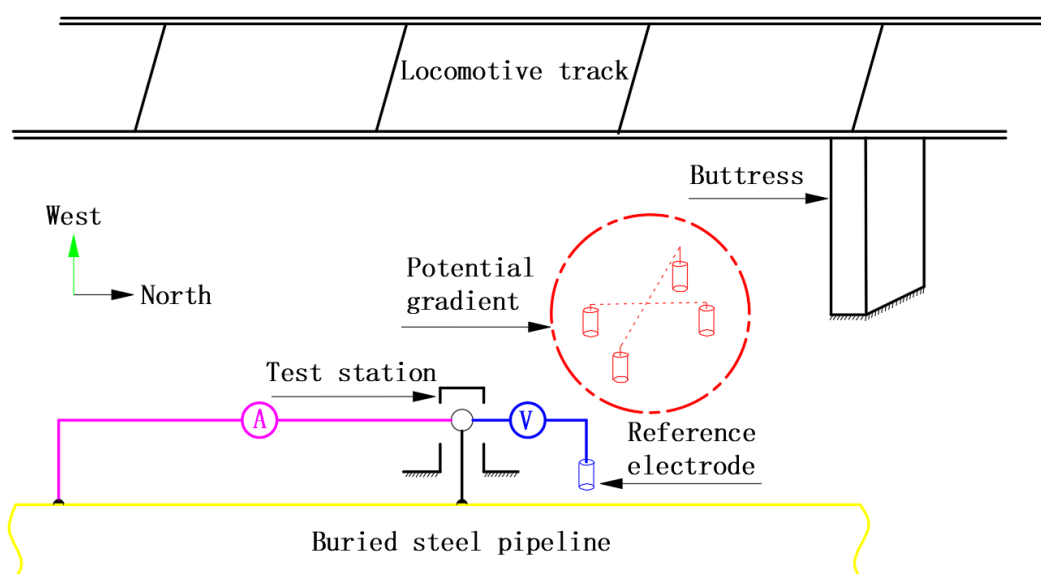


Figure 2. Schematic diagram of the field-testing arrangement

2.3.1 Pipeline-to-soil potential

Before starting the test, a copper sulfate reference electrode is arranged near the abovementioned test field. To minimize the influence of the IR drop on the measurement errors [14, 15], the reference electrode should be buried close to the unmeasured pipeline. In addition, the electrode is buried at a depth of 15 cm. Meanwhile, the bottom of the reference electrode completely contacts the soil, and the soil around the reference electrode is sufficiently moist. During the test time of 17:00~00:10, this device tests the potential between the reference electrode and the pipeline.

2.3.2 Surface potential gradient

The soil of the surface potential gradient is the shifted value of the soil potential per unit length (GB/T19285-2014). With the measuring point as the centre and a distance of 2 metres as the radius, four reference electrodes are arranged uniformly parallel and perpendicular to the pipeline on the circular arc. The vector composition value of the potential difference in the horizontal and vertical directions is measured, which is defined as the potential gradient of the measuring point [13]. Before the test, the reference electrode was buried at a depth of 15 cm. It is worth noting that during the burying process, the bottom of the reference electrode fully contacts the soil, and the soil around the reference electrode is sufficiently moist. The test time was from 17:00 to 00:10, and the variational value of the potential gradient was measured.

2.3.3 Current within the pipeline

Due to the current technical conditions and limitations regarding the development level of the testing equipment, it is very difficult to accurately measure the operating current within the pipeline. With the help of the pipeline test station and the reserved measuring position within the pipeline, 1 ohm of resistance is added between the test station and the reserved position. This work uses the test device to measure the current. It is worth noting that according to the national standard, the distance between the two measuring points is 30 metres. The test time is from 17:00 to 00:10, which includes a period of the rail transit locomotive operation and a period of no operation.

3. RESULTS AND DISCUSSION

3.1 Pipe-to-soil potential testing

Figure.3 shows the measured value of the pipe-to-soil potential measurement during the testing period. According to the acquired data, it is known that during the time from 17:00 to 23:50, the pipe-to-soil potential exhibits a serious fluctuation due to the locomotive operations. The maximum negative and positive amplitude of the potential fluctuate greatly, and the fluctuation range of the potential amplitude ranges from -2.814 V to 1.045 V. There is no interference from the rail transit locomotive during the time from 23:50 to 00:10, the variation range of the measured pipe-to-soil potential amplitude

ranges from -0.869 V to -0.914 V, and the average value is -0.81 V. To analyse the influence of the fluctuating value on the pipe-to-soil potential during rail locomotive operation, the measured data processing is performed from 17:00 to 23:50. The data obtaining from being the interference of the rail transit locomotive minus -0.81 V which is the average pipe-to-soil potential without the interference, thereby obtaining the potential data caused by the rail locomotive operation, and the pipe-to-soil potential shift in the range of -2.004 V to 1.855 V. The fluctuating tendency of the potential caused by interference is shown in Figure.4.

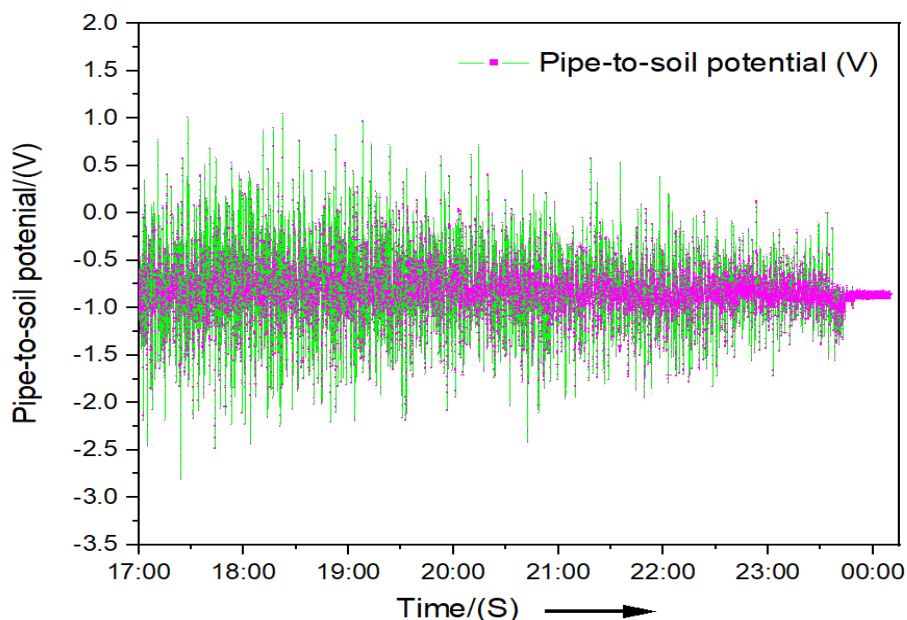


Figure 3. The variation in the measured pipe-to-soil potential with time-dependence

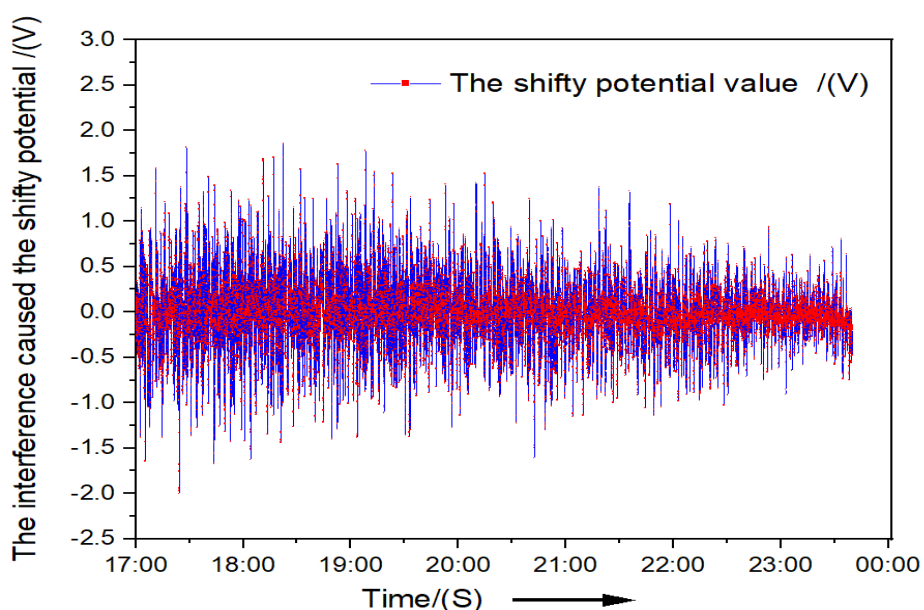


Figure 4. The interference caused the shift in potential to be time-dependent

According to Figure.4, the stray leaking current from the rial buttress has a serious impact on the buried steel pipelines. During the operation of the locomotive, the maximum positive and negative shift values of the potential caused by the locomotive operation are large at the test position, which causes serious interference to the pipeline, thereby causing serious corrosion of the pipeline. Furthermore, the negative and positive shift law of the measured potential fluctuates with the operating timetable of the locomotives, and the shifting law of the potential amplitude presents a positive correlation with the operating frequency of the locomotive. The test result is consistent with the research conclusion of Chen [3]. Meanwhile, the researchers used modeling methods to study pipeline corrosion on the rail transit [16, 17]. The modeling results are similar to the field testing. Furthermore, Other researchers used electrochemical testing methods to study the buried pipeline corrosion, conclusions of which can be used as the guidance for the field testing [18, 19].

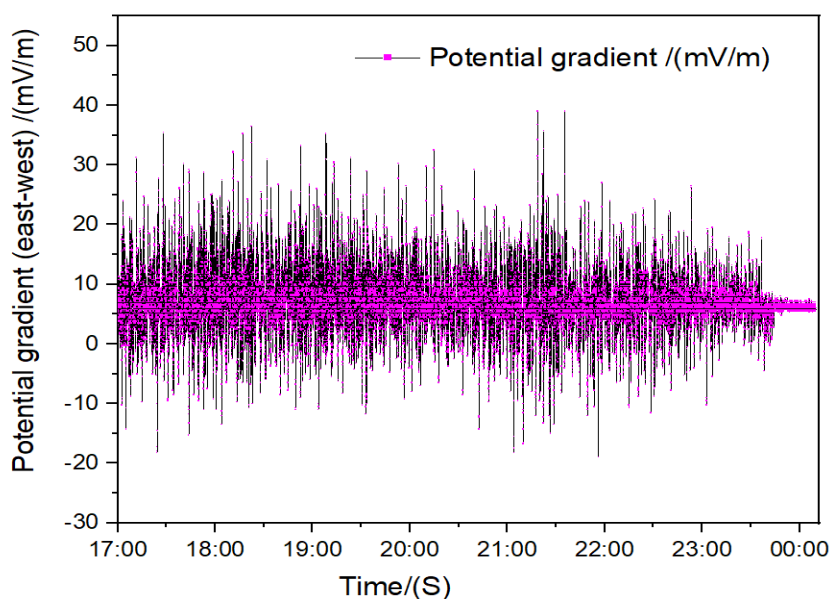


Figure 5. Time-dependent measured potential gradient (east-west)

3.2 Surface potential gradient testing

During the measuring period, the chart depending on the measured data of potential difference from east to west is shown in Figure.5. According to Figure.5, during the time from 17:00 to 23:50, the locomotive operation causes the maximum negative and positive amplitude of the potential difference to be large, and its fluctuation range is from -19 to 39 mV/m. From 23:50 to 00:10, without interference from the rail transit locomotive operation, the fluctuation range of the measured potential difference is from -4.75 to -2.25 mV/m, and the average value is -3.73 mV/m. To further analyse the influence of the rail locomotive on the potential difference during rail locomotive operation, the data obtaining the measured potential difference are processed during the time period from 17:00 to 23:50, and the data coming from rail transit locomotive operation minus -3.73 mV/m which is the average potential value

without rail transit locomotive interference. The processed data is the shifted value of the potential difference caused by rail locomotive interference, the shifted range of the potential difference is from -15.26 to 42.74 mV/m in the east-west direction, and the processed data are drawn as shown in Figure.6.

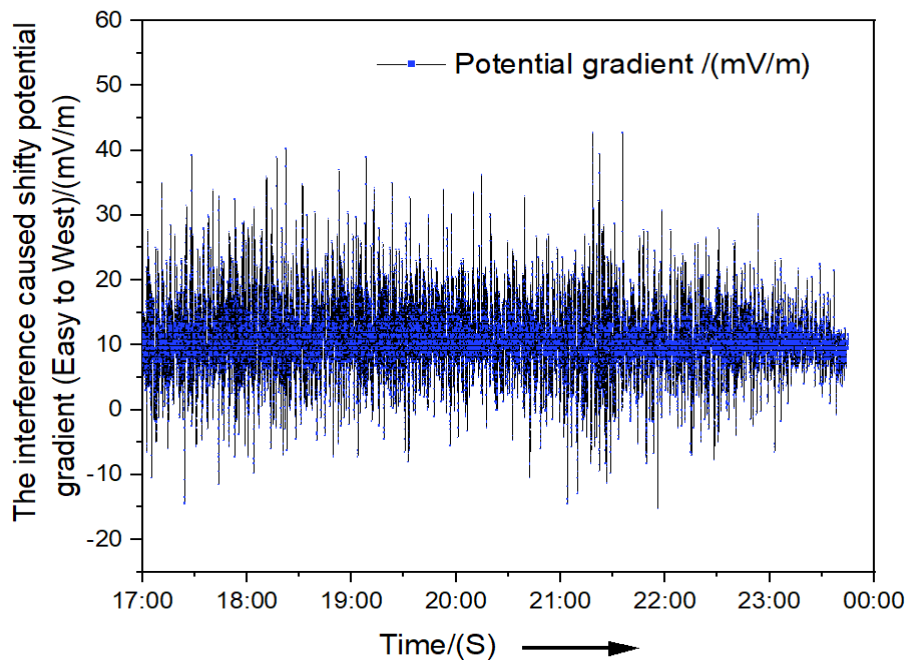


Figure 6. The interference caused shifted potential gradient in a time-dependent (easy-west) manner

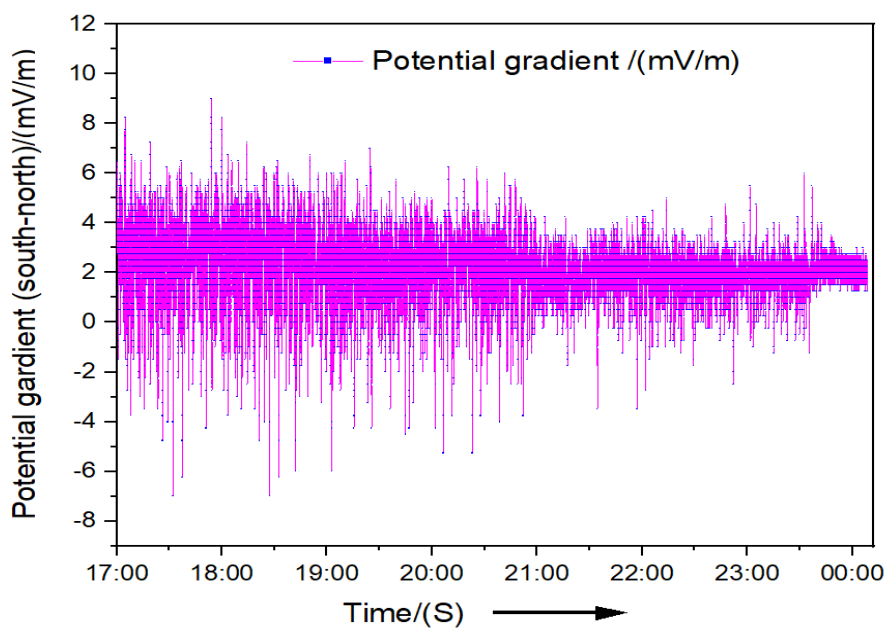


Figure 7. Time-dependent measured potential gradient (south-north)

According to Figure.6, during the operation of rail transit locomotives, the maximum positive and negative shift values of the potential difference caused by rail transit locomotives operation are large at the test point in the east-west direction, and the change law of the proceeded data shows a positive correlation with the running timetable frequency of the rail transit locomotives. The test result is similar to the research conclusion from Chen [3] and Allahkaram [8]. Meanwhile, Other researchers have studied the factors (including soil, water, and sulfate reduction bacteria) that affect the accuracy of field measurements [20, 21], the results of which can be helpful to improve the accuracy of field testing.

During the testing time, Figure.7 shows the chart of the potential difference that comes from the measured data in the south to north direction. According to Figure.7, during the time period from 17:00 to 23:50, due to interference from the locomotive operation, the fluctuation range of the potential difference ranges from -7 to 9.2 mV/m in the north-south direction. Without locomotive operations, the fluctuation range of the measured potential difference is from -4.75 to -2.75 mV/m, and the average value is -3.87 mV/m. The same data processing method as applied in the east-west direction is adopted during the operating time of the locomotive, and a potential shift range from -3.13~13.07 mV/m is obtained in the north-south direction. The processed data is drawn as shown in Figure.8.

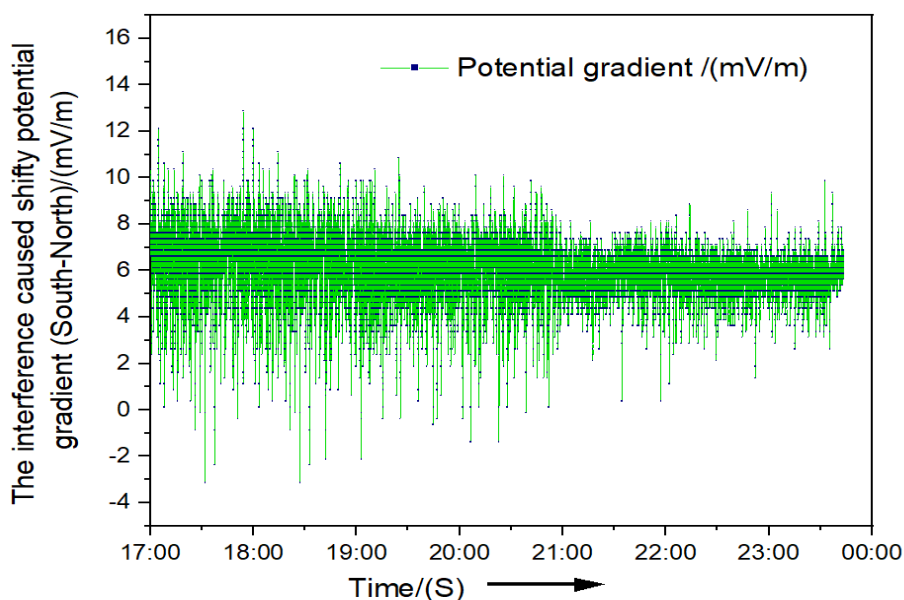


Figure 8. The interference caused shifted potential gradient in a time-dependent manner (south-north)

According to Figure.8, during the operation of locomotives, there is a small variational amplitude range of potential differences in the north-south direction, which is caused by the interference of rail transit at the testing point. The operating frequency of the transit locomotives has a certain positive correlation with the variational potential. The tested result is similar to the research conclusion of Chen [3].

Furthermore, according to Figure.6 and 8, the potential gradient from east to west fluctuates considerably, and the fluctuation law of the potential difference running in the north-south direction is

similar to that following the east-west direction, but the fluctuation deviation value is relatively small in the north-south direction. Therefore, the potential difference in the east-west direction is affected by the leakage current from the rail buttress, which causes the measured potential difference to fluctuate greatly in the east-west direction. The vector synthesis of potential differences between the east-west and south-north directions are shown in Table 1. Figures.6 and 8 and Table 1 show that the average potential gradient is 12.18 mV/m at 30.2 degrees in the southeast.

Furthermore, the measured potential difference data are classified in the east-west and south-north directions. The measuring time is drawn with 1 second as the time unit, and the east-west and north-south data are used as the horizontal and vertical axes, respectively. The position of the vector composition point of the surface potential gradient is shown in Figure.9.

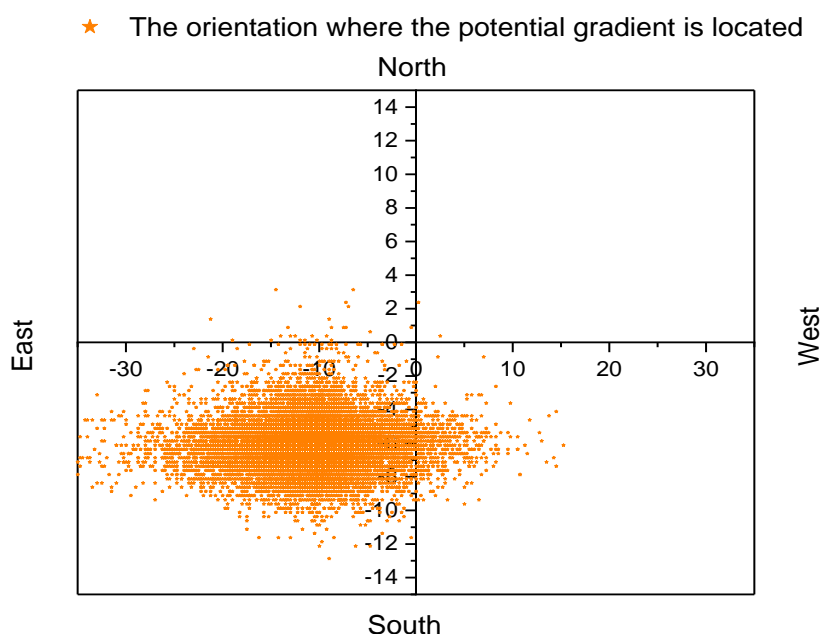


Figure 9. The position of vector composition points of the surface potential gradient

Table 1. The interference caused the fluctuation of the potential gradient

	East-West (mV/m)	South-North (mV/m)	Surface potential gradient(mV/m)	Tangent value of angle (East-West)
Mean value	10.53	6.13	12.18	0.582
Maximum value	42.74	13.07		
Minimum value	-15.26	-3.13		

It is known from the distribution position of the potential gradient in Figure. 9 that the leaking current flows to the test point mostly along the southeast direction. It can be seen from the location distribution of the test points that the test point is located southeast of the rail buttress, and the direction of the potential gradient obtained by the test is consistent with the relative direction between the

measured pipe-section and the buttress. Therefore, it can be judged that the leaking current from the rail buttress flows towards the measured pipe section, thereby causing the pipeline to be corroded during locomotive operation.

3.3 Current within the pipeline testing

The chart of the current within the pipeline is shown during the measurement period in Figure.10. Due to the operation of the rail locomotive, it can be seen from Figure.10 that the range of the current amplitude is from -49 mA to 28 mA during the time period from 17:00 to 23:50. Without interference from the rail locomotive operations in the time ranging from 23:50 to 00:10, the measured range of the current amplitude is from -11 mA to -8 mA, and the average value is -9 mA.

To further analyse the influence of the current flowing into and out of pipelines on the pipeline corrosion, the measured current is divided into the positive and negative currents during the measured time from 17:00 to 23:50. The positive current data indicate that the current flows from the pipeline to the soil. However, negative current data suggest that the current flows from the soil to the pipeline. After the premeasured data are classified, it is known that the fluctuation range of the positive current ranges from 0 to 37 mA, and the average value is 6.5 mA. The negative current fluctuation ranges from -40 to -1 mA and the average value is -5.0 mA. The classified positive and negative current data are drawn as shown in Figures 12 and 13, respectively.

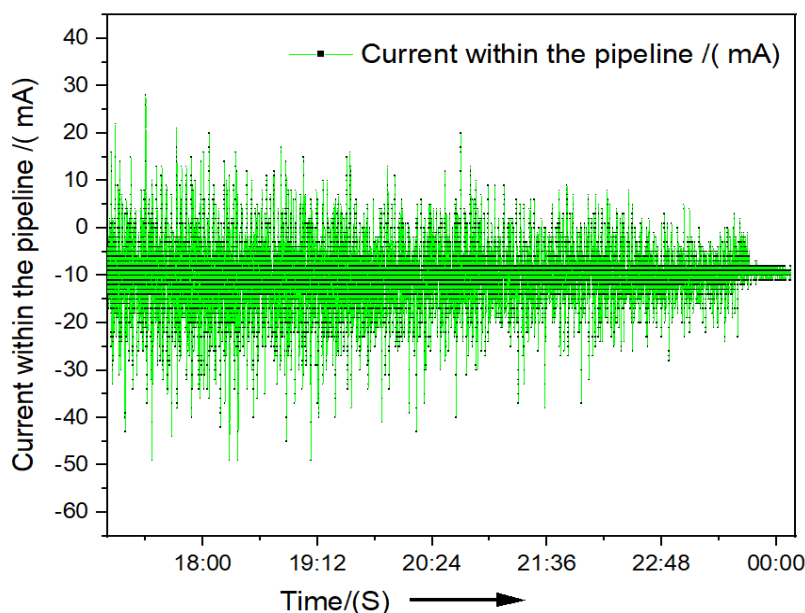


Figure 10. Time-dependent measured acquired current within the pipeline

To analyse the influence of the leaking current on the gas pipeline, during the test time of 17:00-23:50, the current variational value is in the range of -40 to 37 mA. When using the abovementioned

processing method to obtain the proceeding data caused by the locomotive operation, the processed data can be drawn as shown in Figure .11.

Furthermore, by classifying the data of the positive and negative currents, it is found that the positive current accounts for 12%, and the negative current accounts for 88%. From the data, it can be seen that the current mainly flows into the pipeline at the measuring point. The specific accounting is shown in Figure.14. However, from the acquired data, it is found that due to the interference of the rail locomotive, the current flowing into the pipeline inevitably flows out of the pipeline from other damaged points of the pipeline, resulting in the pipeline being corroded at points where the anti-corrosion coating is damaged, thereby inducing pipeline leakage accidents. Therefore, it is known that the operation of the rail locomotive has a strong influence on the corrosion of the buried pipeline near the rail buttress. Currently, some researchers have studied pipeline corrosion caused alternating current (A.C.) on buried steel pipelines near the rail buttress [22, 23]. Furthermore, the degree of pipeline corrosion was compared to alternating current-direct current. The result shows that the D.C. corrosion is stronger than A.C. Therefore, it is necessary to regularly measure the leaked current within the pipeline from D.C. driving rail transit [24].

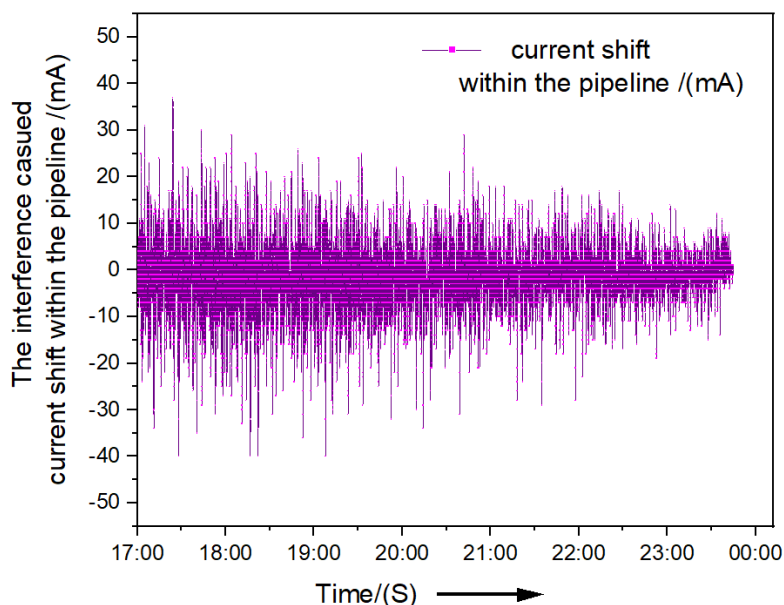


Figure 11. The interference caused current shifts within the pipeline

3.4 Protective measures

Based on the abovementioned measured data, it is found that the operation of rail transit locomotives will have a great impact on the corrosion of buried steel pipelines near rail buttresses. Necessary measures must be taken to prevent pipeline corrosion from developing [25, 26]. Adding a smart monitoring system to the pipeline sacrificial anode device can be used to acquire the state parameters of the sacrificial anode in time, thereby replacing the sacrificial anode in time. Then, the

insulated joint is installed in the new pipe section to avoid the current flowing long distances inside the pipeline [27, 28]. Finally, a drainage device can be installed on the pipeline near the rail buttress to quickly discharge the current within the pipeline to the external device receiving the current.

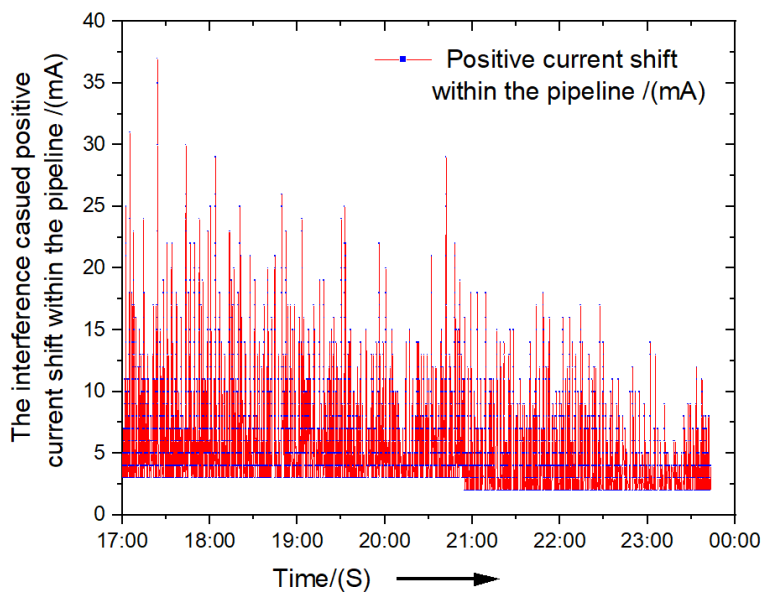


Figure 12. The interference caused a positive shifting current within the pipeline

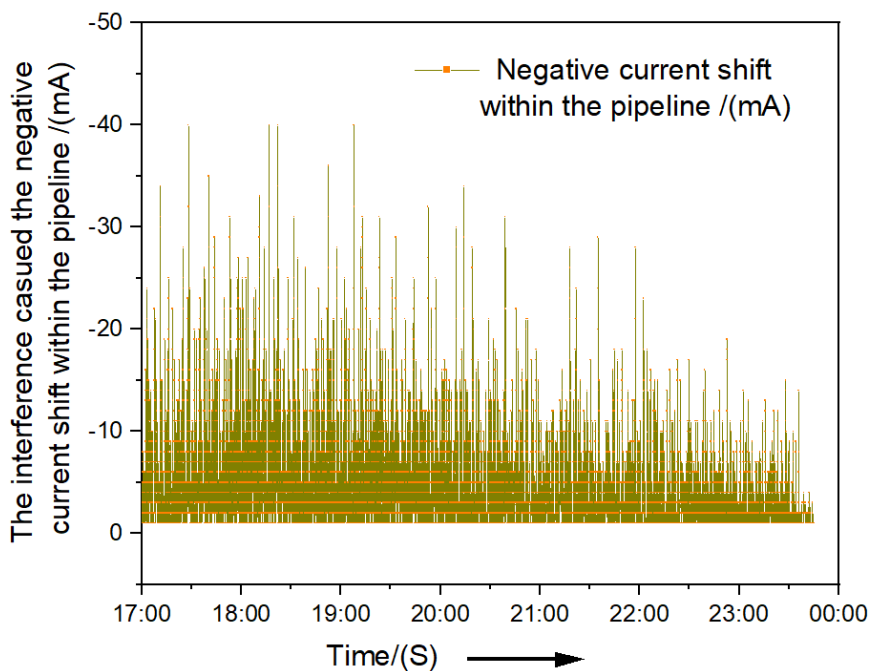


Figure 13. The interference caused a negative shifting current within the pipeline

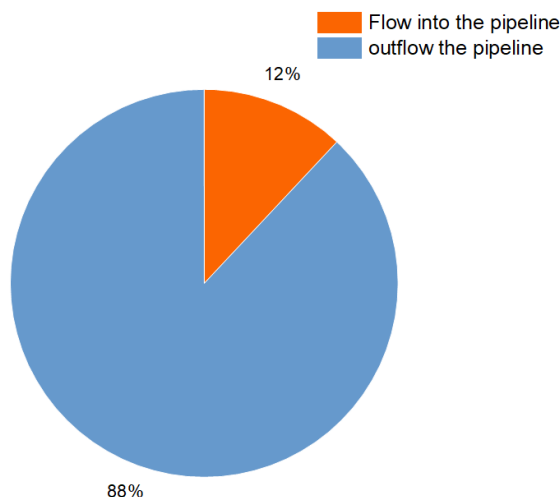


Figure 14. The proportions of the positive and negative currents from rail buttress leakage

4. CONCLUSIONS

In this work, a novel test device was used to conduct field testing on the corrosion interference of buried pipelines located near the rail buttress. Based on the abovementioned tested data, the following conclusions were obtained.

(1) During rail transit operation, the leaking current from the rail buttress has a strong corrosive influence on buried steel pipelines and accelerates their corrosion.

(2) By measuring the current within the pipeline on the target pipe-section, it is found that 88% of the current coming from the rail buttress flows into the pipeline. A large amount of current flowing into the pipeline accelerates the development of pipeline corrosion, resulting in annual losses to weight and annual additions to the corrosion thickness of the steel pipelines increasingly.

(3) The work proposes adding a smart monitoring system, insulation joints, and drainage device near the rail buttress to minimize pipeline corrosion and prevent pipeline leakage accidents.

ACKNOWLEDGMENT

The authors are grateful for the support from the Subtopics of Key Technologies Research and Development Program (NO.2016YFC0802404). We also appreciate all the reviewers and editors for their professional and constructive comments.

CONFLICTS OF INTEREST

There are no conflicts to declare.

References

1. X. J. Shen, X. C. Jiang, *IET. Gener. Transm. Dis.*, 5 (2011)720.
2. G. Lucca, *Electr. Eng.*, 103(2020) 417.

3. C. Wang, L. Wei, *Int. J. Electrochem. Sci.*, 13 (2018) 1700.
4. Z. Chen, C. Qin, J. Tang, Y. Zhou, *J. Nat. Gas. Sci. Eng.*, 15 (2013) 76.
5. M. Wasim, S. Shoaib, N. M. Mubarak, Inamuddin, A. M. Asiri, *Environ. Chem. Lett.*, 16 (2018) 861.
6. D. Paul, *IEEE. Ind. Appl. Mag.*, 22 (2016) 8.
7. Z. Chen, D. Koleva, K. van Breugel, *Corros. Rev.*, 35 (2017) 397.
8. S. R. Allahkaram, M. Isakhani-Zakaria, M. Derakhshani, M. Samadian, H. Sharifi-Rasaey, A. Razmjoo, *J. Nat. Gas. Sci. Eng.*, 26 (2015) 453.
9. Y. Hong, Z. Li, G. Qiao, J. Ou, *Constr. Build. Mater.*, 157 (2017) 416.
10. Z. G. Chen, C. K. Qin, Y. J. Zhang, J. X. Tang, *Adv. Mater. Res.*, 239-242 (2011) 1219.
11. A. Ogunsola, A. Mariscotti, L. Sandrolini, *IEEE Trans. Power Deliv.*, 27 (2012) 2238.
12. X. Peng, Z. Huang, B. Chen, D. Liu, H. Li, *Eng. Fail. Anal.*, 116 (2020) 104760.
13. SAC, GB/T19285-2014., (2014)1.
14. W. Oelßner, F. Berthold, U. Guth, *Mater. Corros.*, 57 (2006) 455.
15. U. M. Angst, M. Büchler, *J. Pipeline Syst. Eng. Pract.*, 9 (2018) 04017035.
16. Z. Cai, X. Zhang, J. Zhang, *J. Electrochem. Sci.*, 15 (2020) 6629.
17. I. M. Gadala, M. Abdel Wahab, A. Alfantazi, *Mater. Des.*, 97 (2016) 287.
18. J. Wang, Z. Li, C. Kong, Z. Yang, J. Liu, G. Cui, *J. Electrochem. Sci.*, 13 (2018) 12099.
19. Q. Ding, Z. Li, D. Dilimulati, D. Wang, X. Shi, *J. Electrochem. Sci.*, 16 (2021) 131063.
20. T. H. Shabangu, A. A. Ponnle, K. B. Adedeji, *12th. IEEE. ICGIAR.*, 1 (2015)1.
21. A. J. Spark, D. W. Law, L. P. Ward, I. S. Cole, A. S. Best, *Environ. Sci. Technol.*, 51 (2017) 8501.
22. Y. Guo, H. Tan, D. Wang, T. Meng, *Anti-corros. Method. M.*, 64 (2017) 599.
23. X. H. Wang, G. Y. Yang, H. Huang, Z. Chen, L. M. Wang, *Appl. Mech. Mater.*, 263-266 (2013) 448.
24. Z. Zhang, P. Gao, Y. Dan, G. Liu, R. Xiang, J. Zou, *J. Electrochem. Sci.*, 13 (2018) 11974.
25. W. S. Sum, K. H. Leong, L. P. Djukic, T. K. T. Nguyen, A. Y. L. Leong, P. J. Falzon, *Plast. Rubber. Compos.*, 45 (2016) 81.
26. L. Dikmarova, V. Nichoga, P. Dub, *IEEE. T. Instrum. Meas.*, 51 (2002) 92.
27. D. Kim, L. Udpa, S. Udpa, *Mater. Lett.*, 58 (2004) 2102.
28. C. Ramella, G. Canavese, S. Corbellini, M. Pirola, M. Cocuzza, L. Scaltrito, S. Ferrero, C. F. Pirri, G. Ghione, V. Rocca, A. Tasso, A. D. Lullo, *J. Pet. Sci. Eng.*, 133 (2015) 771.